ANL-ART-189
ANL-METL-23

Thermal Hydraulic Experimental Test Article – Status Report FY20 Q2

Nuclear Sciences and Engineering Division

About Argonne National Laboratory

Argonne is a U.S. Department of Energy laboratory managed by UChicago Argonne, LLC under contract DE-AC02-06CH11357. The Laboratory's main facility is outside Chicago, at 9700 South Cass Avenue, Argonne, Illinois 60439. For information about Argonne
and its pioneering science and technology programs, see www.anl.gov.

DOCUMENT AVAILABILITY

Online Access: U.S. Department of Energy (DOE) reports produced after 1991 and a growing number of pre-1991 documents are available free at OSTI.GOV (http://www.osti.gov/), a service of the US Dept. of Energy's Office of Scientific and Technical Information.

Reports not in digital format may be purchased by the public from the National Technical Information Service (NTIS):

U.S. Department of Commerce
National Technical Information
Service 5301 Shawnee Rd
Alexandria, VA 22312
www.ntis.gov
Phone: (800) 553-NTIS (6847) or (703) 605-6000
Fax: (703) 605-6900
Email: **orders@ntis.gov**

Reports not in digital format are available to DOE and DOE contractors from the Office of Scientific and Technical Information (OSTI):

U.S. Department of Energy
Office of Scientific and Technical Information
P.O. Box 62
Oak Ridge, TN 37831-0062
www.osti.gov
Phone: (865) 576-8401
Fax: (865) 576-5728
Email: **reports@osti.gov**

Disclaimer

This report was prepared as an account of work sponsored by an agency of the United States Government. Neither the United States Government nor any agency thereof, nor UChicago Argonne, LLC, nor any of their employees or officers, makes any warranty, express or implied, or assumes any legal liability or responsibility for the accuracy, completeness, or usefulness of any information, apparatus, product, or process disclosed, or represents that its use would not infringe privately owned rights. Reference herein to any specific commercial product, process, or service by trade name, trademark, manufacturer, or otherwise, does not necessarily constitute or imply its endorsement, recommendation, or favoring by the United States Government or any agency thereof. The views and opinions of document authors expressed herein do not necessarily state or reflect those of the United States Government or any agency thereof, Argonne National Laboratory, or UChicago Argonne, LLC.

ANL-ART-189
ANL-METL-23

Thermal Hydraulic Experimental Test Article – Status Report FY20 Q2

M. Weathered, D. Kultgen, E. Kent, C. Grandy, T. Sumner, A. Moisseytsev, T. Kim

Nuclear Sciences and Engineering Division
Argonne National Laboratory

April 2020

TABLE OF CONTENTS

1. Executive Summary 1
2. Introduction 2
   2.1. System Overview and Systems Code Application 3
3. Primary Vessel Component Summary 5
   3.1. Primary Flange and Inner Vessel 6
   3.2. Instrumentation 16
   3.3. Intermediate Heat Exchanger 23
   3.4. Submersible Flowmeter 29
   3.5. Pump 30
   3.6. Immersion Heater 37
4. Secondary Sodium Component Summary 40
   4.1. Sodium-to-Air Heat Exchanger 41
   4.2. Secondary Sodium Piping 44
5. Water Testing 45
6. THETA Model Development 50
7. Conclusions and Path Forward 51
8. Acknowledgements 51
9. References 52

LIST OF FIGURES

Figure 1 – THETA Primary Heat Transport System (28 inch test vessel not shown) 2
Figure 2: Isometric drawing of THETA primary vessel and secondary system left. Location of THETA in METL facility highlighted with red square, right. 2
Figure 3: P&ID schematic of THETA 3
Figure 4: THETA pool and core geometry. Core nominal diameter: 0.2 [m] (8”), core heated length: 0.3 [m] (12”) see heater geometry in Figure 41 for more information 4
Figure 5: Schematic of SAS4A/SASSYS-1 showing locations of various compressible volumes (CV#) and segments (S#) 5
Figure 6: THETA primary vessel components 6
Figure 7: 28”, 400# ANSI flange, THETA primary system 7
Figure 8: A-frame test article ‘flipper’, left. Bearing with gear box used to rotate flange 360 degrees. 7
Figure 9: THETA primary flange mounted to flipper, positioned 90 degrees to the horizontal showing the wetted raised face 8
Figure 10: Initial installation of inner vessel on primary flange 8
Figure 11: Penetration of centrifugal pump shaft through bottom of inner vessel. As can be seen the initial lineup of the pump shaft to the vessel penetration was not centered. . 9
Figure 12: Installation of primary flange on CNC mill machine 10
Figure 13: Confirming flatness of primary flange raised face to ensure parallelism with CNC mill x-y plane 10
Figure 14: Dial indicating difference in elevation between raised face of primary 28” flange to each auxiliary flange raised faces 11
Figure 15: 8” Flange, left. 5” flange, middle. 4” flange, right. 11
Figure 16: Primary flange nameplate 11
Figure 17: Drawing showing inner vessel offset from flange to illustrate support rod mounting location for inner vessel, top, mounting locations with studs installed in primary flange for support rods, bottom. 13
Figure 18: Primary flange positioned to bore 3X holes for 5/8” -11 STI tap for Nitronic-60 helicoil thread inserts to mount inner vessel support shafts 14
Figure 19: Inner vessel mounted to CNC machine for modifications 14
Figure 20: Photo from inside the bottom of the inner vessel looking up towards the primary flange, the support shafts, intermediate heat exchanger shell and column pipe for the centrifugal pump are visible 15
Figure 21: Photo of THETA after dry assembly and prepared for water testing 16
Figure 22: THETA instrumentation port locations 18
Figure 23: Multi-junction TC positions for ports 4, 6, and 9, hot pool sodium shown with translucent yellow for reference. 18
Figure 24: Multi-junction TC probe installed in port #6, left. Multi-junction TC probe installed in port #4, right. 19

Figure 25: Dry fitting of THETA cold pool components in preparation for testing in deionized water. Multi-junction TC probes installed in ports # 4, 6, and 9 can be seen. 19
Figure 26: Photo showing 150 µm OD silica optical fiber 20
Figure 27: Optical fiber capillaries mechanically coupled to 1/4" multi-junction thermocouples 21
Figure 28: View of 3 optical fiber capillaries coupled to 1/4" multipoint thermocouple probes 21
Figure 29: Sprung bellows to makeup thermal expansion differential of 1/16" capillaries, left. High temperature Inconel spring photo, right 22
Figure 30: Sprung bellows adapter installed in port #7 22
Figure 31: Shell and tube intermediate heat exchanger 23
Figure 32: Drawings showing IHX baffle plate and tube bundle upcomer 23
Figure 33: IHX predicted shell side temperature differential and thermal power dissipation as a function of shell side flow rate 25
Figure 34: IHX Outlet dimension, top. Isometric model of variable elevation IHX outlet, bottom left. Drawing showing predicted cold pool temperature distribution as a function of IHX outlet window elevation, (red = hot, purple = warm, blue = cold), bottom right. 27
Figure 35: Variable elevation IHX outlet. Drawings showing the inner barrel, left, outer barrel, middle, and the assembly of inner/outer barrel and actuator stem, right. 28
Figure 36: Photo showing the IHX outlet inner barrel, left, and the outer barrel, right 28
Figure 37: Submersible permanent magnet flowmeter 29
Figure 38: Photo of the THETA submersible permanent magnet flowmeter 29
Figure 39: Flowmeter induced voltage vs flow rate for THETA submersible electromagnetic flowmeter, [1] 30
Figure 40: Pump as delivered, left, 4.5" OD impeller, right 30
Figure 41: Pump curves made using water at 27 °C as surrogate fluid. System curves shown for primary and secondary sodium. 31
Figure 42: Photo showing the air-to-sodium seal for the THETA centrifugal pump. Shown from left to right: packing block, lantern ring, follower. 31
Figure 43: Photo showing the 5" 300# ANSI flange with graphite gasket in place in preparation for installation of packing block. Nitronic-60 helicoil thread adapters are installed in all threads to reduce likelihood of galling. 32
Figure 44: Photo showing the packing block cavity. On the right can be seen a single layer of graphite packing. Two holes are bored radially into the cavity, the lower one shown is for inert gas pressurization of the lantern ring void, the upper bore is for an 1/8" thermocouple to monitor packing temperatures during operation. 32
Figure 45: Photo showing the wetted face of the pump flange along with the thrower that acts to centrifugally deposit debris falling from the packing block into the debris well. Also notice the ethanol, this is sprayed onto lint-free lab wipes and used to ensure cleanliness of all components before testing. 33

Figure 46: Photo showing the 5” 300# mounting flange on the THETA primary flange. The energized spring seal groove can be seen on the raised face. A debris well can be seen which acts to catch any dust or large particles that may fall from the graphite packing seal. 33
Figure 47: Photo showing the packing block installed with the debris well below. 34
Figure 48: Photo showing the centrifugal pump case with labyrinth seal lower plate and shaft adapter. 34
Figure 49: Photo showing the labyrinth seal shaft adapter 35
Figure 50: Photo showing the installation of the centrifugal pump shaft and upper bearing assembly into THETA. 35
Figure 51: Photo showing the bottom side of the inner vessel, pump case is not installed so the labyrinth plate and pump impeller are visible 36
Figure 52: Photo showing the underside of the inner vessel with pump case and piping installed 36
Figure 53: 4.5” Diameter 316SS 3D printed impeller by Oak Ridge National Laboratory, [9] 37
Figure 54: Chromalox 38 kW Immersion Heater (top). Heater control system electrical enclosure (bottom). 38
Figure 55: Photo showing the installation of the THETA immersion heater. 39
Figure 56: Photo showing two of the four thermocouples welded to the hairpin heaters at the bottom of the immersion heater 39
Figure 57: Photo showing the shroud that surrounds the immersion heater in the cold pool to form the core flow path 40
Figure 58: Isometric 3D drawing showing THETA secondary system without (top) and with (bottom) 2” of insulation 41
Figure 59: Photo of the sodium-to-air heat exchanger as received from the manufacturer 42
Figure 60: CAESAR operating scenarios showing vessel, AHX, expansion tank, piping temperatures 45
Figure 61: 260 gallon polypropylene vessel for THETA water testing, left. Dip tube for transferring DI water between the intermediate bulk container and the polypropylene vessel, right. 46
Figure 62: 275 gallon intermediate bulk container of deionized water, left. Self-priming pump and valve manifold for transferring water between the intermediate bulk container and the test vessel. 46
Figure 63: Manifold for ultraviolet sanitization of DI water to eliminate biological contamination. Water may be directed and through the UV cartridge with the UV Throttle Valve. The valve may be throttled to <=6GPM to ensure sufficient residency time of the flowing water to eliminate contaminates. A 0-10 GPM flowmeter is positioned in line with the UV cartridge circuit. 47
Figure 64: Photo of THETA bottom assembly ready for water testing, a Blancett PN B110-875 turbine mechanical flowmeter will be used for water testing, shown installed at the bottom with yellow colored waterproof data cable connected. 48

Figure 65: THETA installed in polypropylene vessel with all thermocouple instrumentation attached, left. Completed water UV purification system and 275-gallon intermediate bulk container, right. 49
Figure 66: THETA pump shakedown preliminary results for flow rate as a function of pump speed. Water at room temperature (no immersion heater). Note that this data was taken without the shaft portion of the labyrinth seal installed, only the case lower plate portion, Figure 48. 49

LIST OF TABLES

Table 1: Primary flange, auxiliary flange nominal dimensions (distance between raised faces), as built dimension and difference of nominal and as built. 12
Table 2: Calculated minimum thickness of each auxiliary flange to satisfy ASME BPVC..... 12
Table 3: THETA instrumentation and measurement. Port positions provided in Figure 25 17
Table 4: ODISI 6104 spatial resolution and measurement rate 20
Table 5: Intermediate heat exchanger sizing parameters 25
Table 6: Sodium-to-Air heat exchanger specification sheet 43

1. Executive Summary

The Thermal Hydraulic Experimental Test Article (THETA) is a facility that will be used to develop sodium components and instrumentation as well as acquire experimental data for validation of reactor thermal hydraulic and safety analysis codes. The facility will simulate nominal conditions as well as protected/unprotected loss of flow accidents in a sodium-cooled fast reactor (SFR). High fidelity distributed temperature profiles of the developed flow field will be acquired with Rayleigh backscatter based optical fiber temperature sensors. The facility is being designed in partnership with systems code experts to tailor the experiment to ensure the most relevant and highest quality data for code validation.

THETA is comprised of a traditional primary and secondary system. The primary system is submerged in the pool of sodium and consists of a pump, electrically heated core, intermediate heat exchanger, and connected piping and thermal barriers (like a redan). The secondary system, located outside of the sodium pool, consists of a pump, sodium to air heat exchanger, and connected piping and valves.

Figure 1 illustrates the main components of the primary system. THETA will be installed in the Mechanisms Engineering Test Loop (METL) with the primary system in the 28 inch Test Vessel #4, Figure 2.

The design work for the facility has been completed, most primary component have been fabricated, primary components are being assembled in preparation for initial testing, and procurement is continuing with the secondary system components. Since the FY19 THETA status report, [1], The THETA primary system components are at Argonne National Laboratory (ANL) and have been dry assembled. The secondary sodium system for heat rejection from intermediate heat exchanger has all been analyzed according to ASME code. All secondary side piping, fittings and a U-stamped air-to-sodium heat exchanger has been procured.

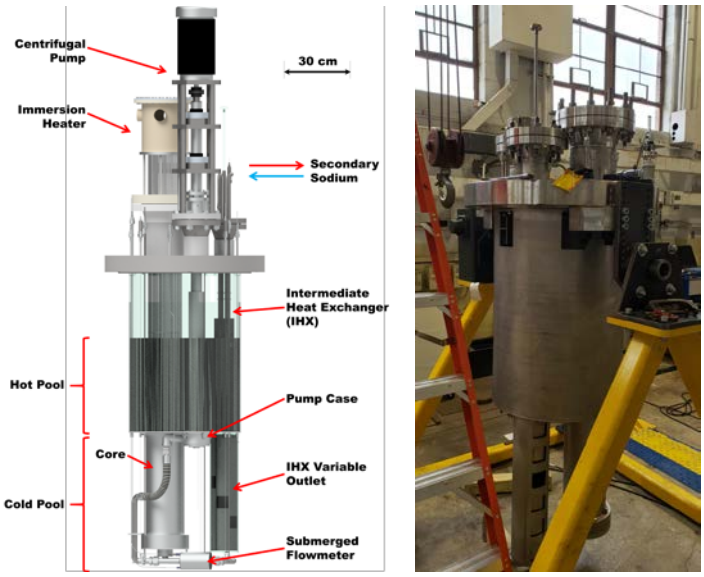

Figure 1 – THETA Primary Heat Transport System (28 inch test vessel not shown)

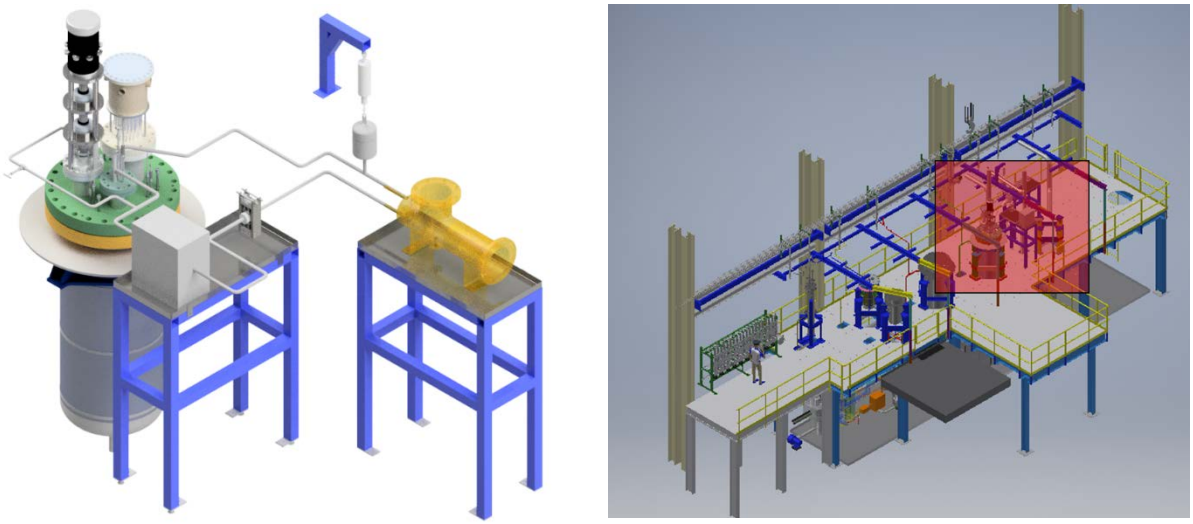

Figure 2: Isometric drawing of THETA primary vessel and secondary system left. Location of THETA in METL facility highlighted with red square, right.

2. Introduction

The Thermal Hydraulic Experimental Test Article (THETA) is a METL vessel experiment designed for testing and validating sodium fast reactor components and phenomena. THETA has been scaled using a non-dimensional Richardson number approach to represent temperature distributions during nominal and loss of flow conditions in a sodium fast reactor (SFR), this analysis was detailed in the THETA FY19 report [1]. The facility is being constructed with versatility in mind, allowing for the installation of various immersion heaters, heat pipes, and heat exchangers without significant facility modification. THETA is being designed in collaboration

with systems code experts to inform the geometry and sensor placement to acquire the highest value code validation data.

2.1. System Overview and Systems Code Application

THETA possesses all the major thermal hydraulic components of a pool type sodium cooled reactor. Figure 3 shows the piping and instrumentation diagram (P&ID) for the primary and secondary sodium circuit. A cross section of the primary vessel shows the pool and core geometry, Figure 4. As can be seen, a 28" METL test vessel is used for the primary sodium "reactor" vessel. An isometric model of the primary/secondary vessels, inter-vessel piping, and air-to-sodium heat exchanger (AHX) can be found in Figure 2.

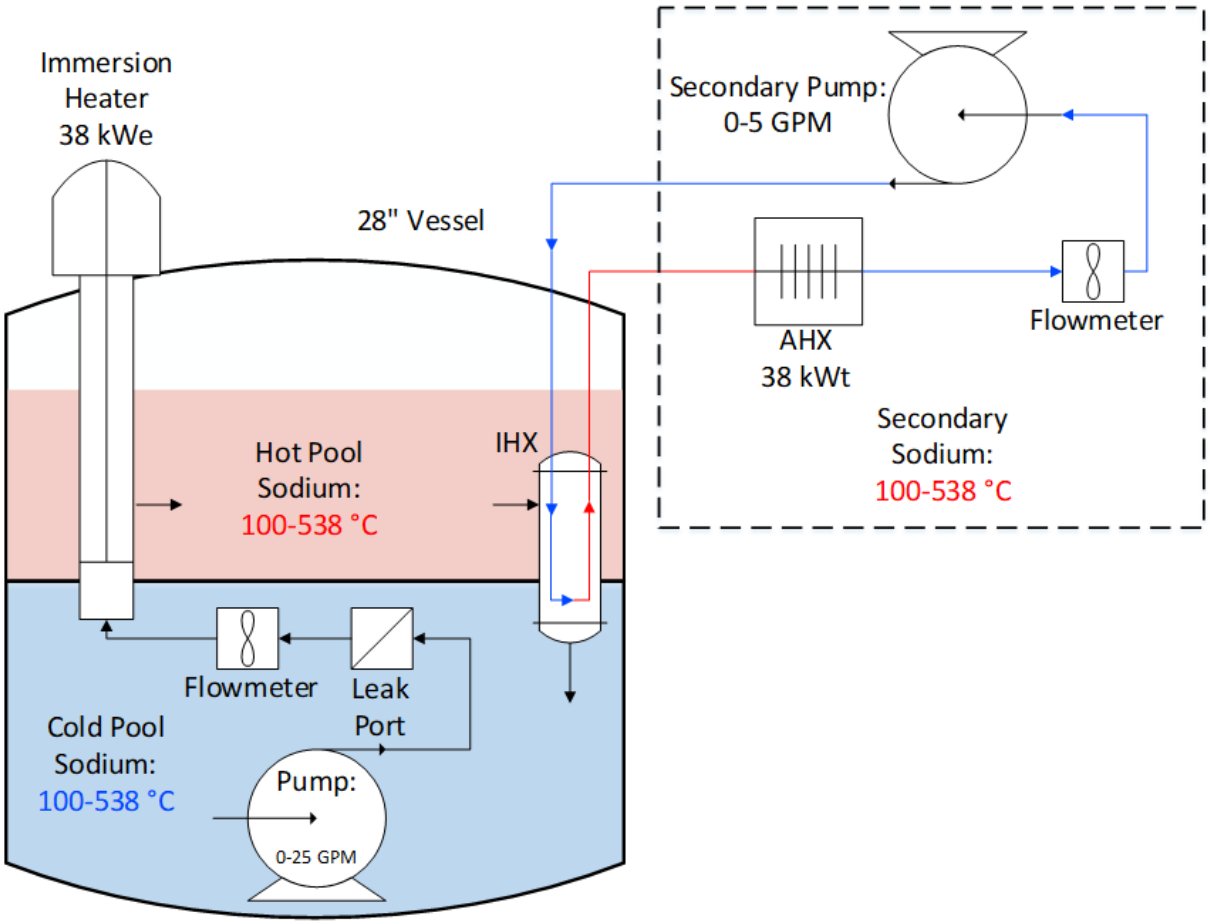

Figure 3: P&ID schematic of THETA

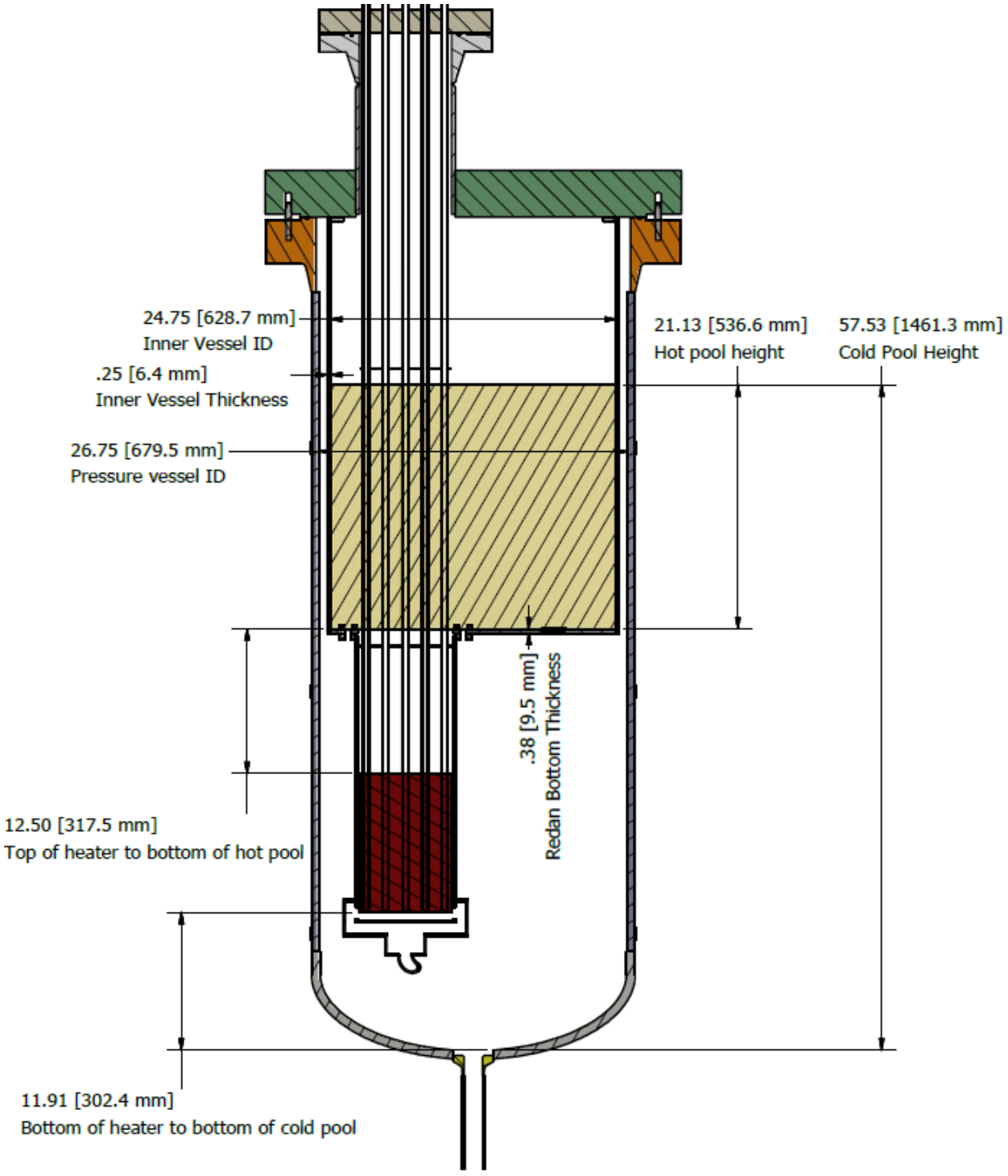

Figure 4: THETA pool and core geometry. Core nominal diameter: 0.2 [m] (8”), core heated length: 0.3 [m] (12”) see heater geometry in Figure 41 for more information

Argonne National Laboratory's SAS4A/SASSYS-1 computer code is used for thermal hydraulic and safety analysis of power and flow transients in liquid metal cooled reactors. Figure 5 gives a graphic displaying the segments and compressible volumes used to perform the deterministic analysis of anticipated events such as protected/un-protected loss of flow reactor trips etc. While SAS4A/SASSYS-1 was benchmarked against tests in historic reactors, such as EBR-II [2], a modern liquid metal thermal hydraulic facility is required for further system's code validation.

A parameter of interest is the differential in elevation between the intermediate heat exchanger (IHX) outlet and the core outlet. This differential will dictate the thermal stratification in the cold pool, thus driving the development of particular natural convection phenomena during reactor trips. The natural convection phenomena in the cold pool can then affect the thermal stratification in the reactor hot pool as sodium temperature from compressible volumes (CV) 3-5 (cold pool) will be transmitted to CV 1-2 (hot pool) in the SAS4A/SASSYS-1 computer code.

Please see [1] for an overview of the current systems code modeling efforts as applied to THETA.

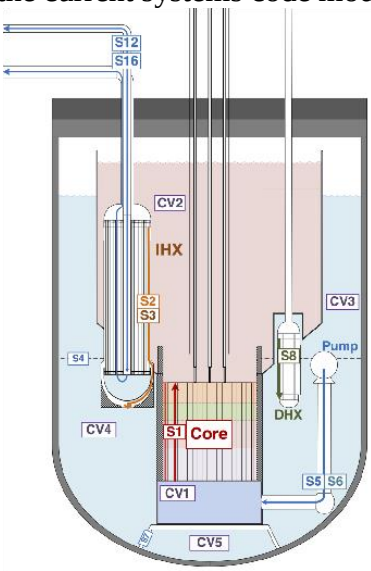

Figure 5: Schematic of SAS4A/SASSYS-1 showing locations of various compressible volumes (CV#) and segments (S#)

3. Primary Vessel Component Summary

The following section presents a summary of all primary vessel components as of April 2020, Figure 6. The primary and inner vessel was receieved early February 2020 and dry assembly and testing of all components has commenced.

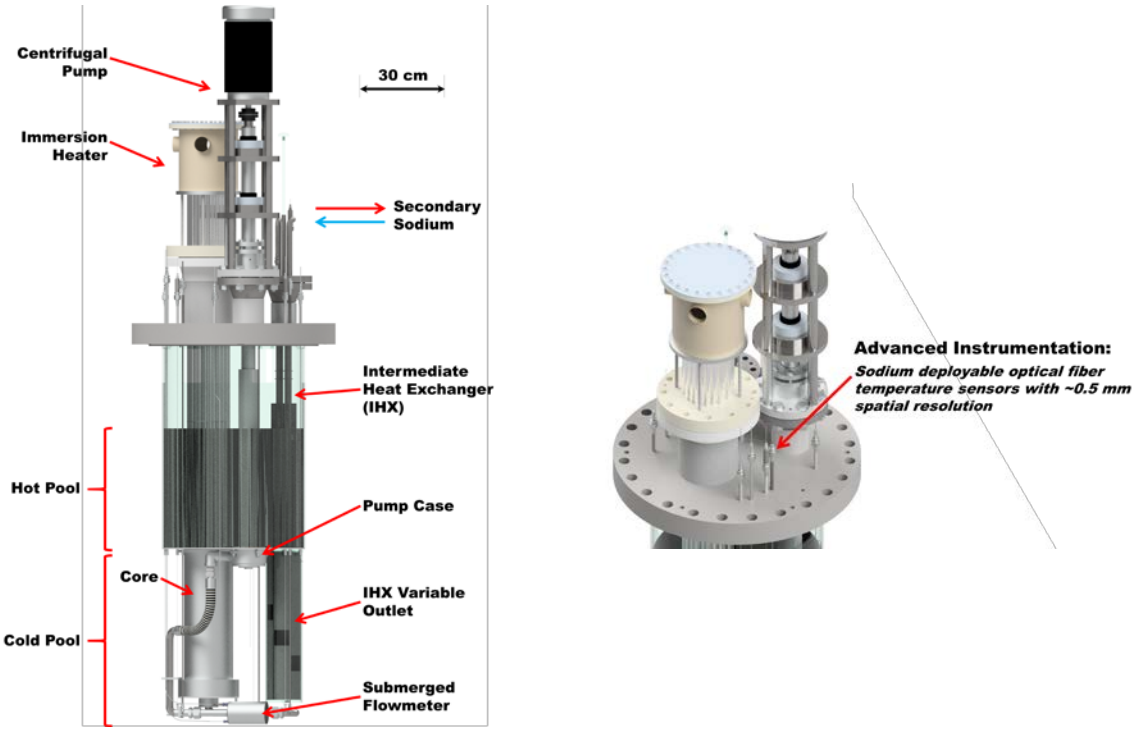

Figure 6: THETA primary vessel components

3.1. Primary Flange and Inner Vessel

The primary, 28" flange was received from the manufacturer in February 2020, Figure 7. A documentation package was also received which included a certificate of conformance to the original build specifications, a final inspection and packing checklist, all material test reports, the ASME data report, a test report from the hydrostatic pressure testing, liquid dye penetrant reports, radiography examination reports and finally, the dimensional inspection drawings.

The maximum allowable working pressure for the primary flange is 100 PSIG at 1200 °F. The minimum design temperature is -320 °F at 100 PSIG. A hydrostatic pressure test was performed on the primary flange at a test pressure of 427 PSIG. A helium leak test was also performed with the flange internals under vacuum with a leak rate ranging from 0.94-1.9 $x10^{-9}$ STD cc/sec.

Figure 7: 28”, 400# ANSI flange, THETA primary system

The primary flange was mounted to the METL test article flipper, a steel A-frame with 2 bearings that mount to a 28” METL test article Figure 8. This allows for fine adjustment of the angle of the flange to facilitate component and instrument installation.

Figure 8: A-frame test article ‘flipper’, left. Bearing with gear box used to rotate flange 360 degrees.

The primary flange can be seen mounted in the flipper and rotated 90 degrees to the horizontal, Figure 9. In this orientation the wetted face was then inspected to ensure surface finish of 32 µin Ra for mating with energized spring seal.

Figure 9: THETA primary flange mounted to flipper, positioned 90 degrees to the horizontal showing the wetted raised face

After mounting the primary pump and immersion heater onto the primary flange, sections 3.5 and 3.6, the inner vessel was then mounted to the primary flange, Figure 10. As can be seen the primary flange was rotated 'upside-down' to allow for careful installation of the inner vessel and to allow for small adjustments to ensure proper clearance for the primary pump shaft through the bottom of the inner vessel.

Figure 10: Initial installation of inner vessel on primary flange

After installation of the inner vessel it was discovered that the three auxiliary flange heights and the cylindricity of the inner vessel side walls were outside of specification, causing interference issues between components and the penetrations in the bottom of the inner vessel, Figure 11.

Figure 11: Penetration of centrifugal pump shaft through bottom of inner vessel. As can be seen the initial lineup of the pump shaft to the vessel penetration was not centered.

In order to remediate these interference issues, the flange was transported to Argonne Central Shops where the flange was placed on a large CNC mill, Figure 12. The 'wetted' flange face was then oriented to be planar with the mill's X-Y plane, and it was confirmed that the flange face met the 0.005" flatness tolerance called out in the original design drawings, Figure 13. The mill z-axis could then be indicated off of the wetted face of the primary flange to determine the heights of the three auxiliary flanges.

Figure 12: Installation of primary flange on CNC mill machine

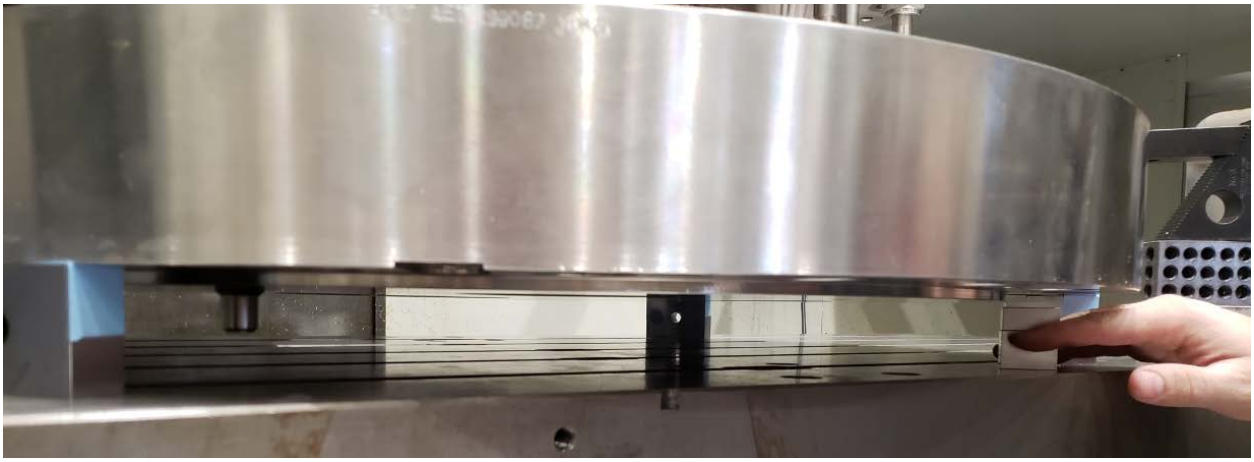

Figure 13: Confirming flatness of primary flange raised face to ensure parallelism with CNC mill x-y plane

The difference in elevation between the 28” flange face and the face of each of the auxiliary flanges were measured at four equidistant locations along the outside of the raised face, Figure 14 and Figure 15. Table 1 provides the nominal (as drawn) dimension, the as-built dimension and the differential from nominal. As can be seen a tolerance of 0.01” was provided for the differential in elevation, the 8” flange was -0.044” out from nominal, the 5” flange was +0.104” out from nominal and the 4” flange was +0.076” out from nominal.

Figure 14: Dial indicating difference in elevation between raised face of primary 28" flange to each auxiliary flange raised faces

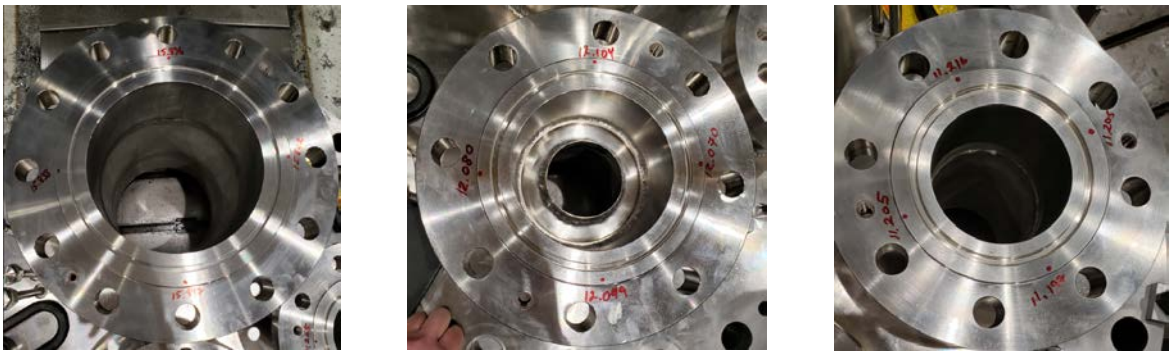

Figure 15: 8" Flange, left. 5" flange, middle. 4" flange, right.

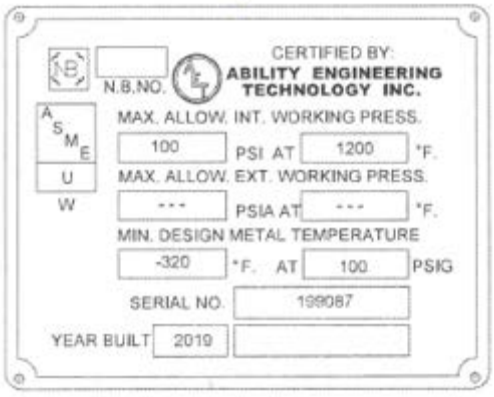

Figure 16: Primary flange nameplate

Table 1: Primary flange, auxiliary flange nominal dimensions (distance between raised faces), as built dimension and difference of nominal and as built.

Flange	Nominal Dimension	As Built	Out from Nominal
8”	15.88 ± 0.01	15.836	-0.044
		15.842	-0.038
		15.847	-0.033
		15.838	-0.042
5”	12.00 ± 0.01	12.104	+0.104
		12.070	+0.070
		12.049	+0.049
		12.080	+0.080
4”	11.14 ± 0.01	11.216	+0.076
		11.205	+0.065
		11.197	+0.057
		11.205	+0.065

Given the 4” and 5” 300# flanges, which mount to the intermediate heat exchanger and primary pump respectively, had face dimensions that were slightly greater than nominal, material could be removed from the raised face of the flange to bring the dimension within tolerance. The 8” flange face distance was closer to the wetted flange than specified in the drawings, therefore material could not be removed from the 8” 300# flange to bring within spec and this flange was not modified. The ASME certified manufacturer of the flange was contacted and asked to provide the minimum calculated thicknesses for the auxiliary flanges to ensure that the flange would still be stamped and rated to the maximum allowable working pressure of 100 PSIG at 1200 °F. The minimum calculated thicknesses for each flange are provided in Table 2.

Table 2: Calculated minimum thickness of each auxiliary flange to satisfy ASME BPVC

Flange	Minimum calculated Thickness to Satisfy Code	Final Thickness After Modification:
4”	0.8264”	1.21”
5”	0.8140”	1.27”
8”	1.0376”	Not Modified

The 4” and 5” flange faces thicknesses were reduced with the mill to bring within specification, Table 1, Table 2. After reducing the flange thicknesses, the energized spring seal grooves were re-machined to the correct specification and the raised face was re-established by removing material from the bolt circle.

A cylindricity of 0.005” was called out in the original design drawings for the inner vessel. A deviation from cylindricity of up to 0.080” was measured on the inner vessel upon inspection at Argonne Central Shops. In order to de-couple the cylindricity of the inner vessel side walls from

the penetration locations in the bottom plate of the vessel, a different inner vessel to primary flange mounting scheme was devised.

As can be seen in Figure 17, qty (3) 1.5” diameter 304 stainless shafts are used to support the inner vessel from the flange. The straightness of the 1.5” shafts may be constrained to a relatively higher tolerance to position the bottom plate of the inner vessel precisely, as compared to relying on the inner vessel side walls for positioning. The qty (3) shafts are attached to the primary flange via 5/8”-11, 316 stainless steel studs. In order to reduce the likelihood of galling occurring between the shafts, studs and flange, Nitronic-60 helicoil inserts were used on all of the threaded connections in this assembly. At the attachment point between the qty (3) shafts and the bottom plate of the inner vessel, X diameter holes were bored and 3/8” thick washer plates are sandwiched on either side to seal the gap between the 5/8” studs and the oversized holes.

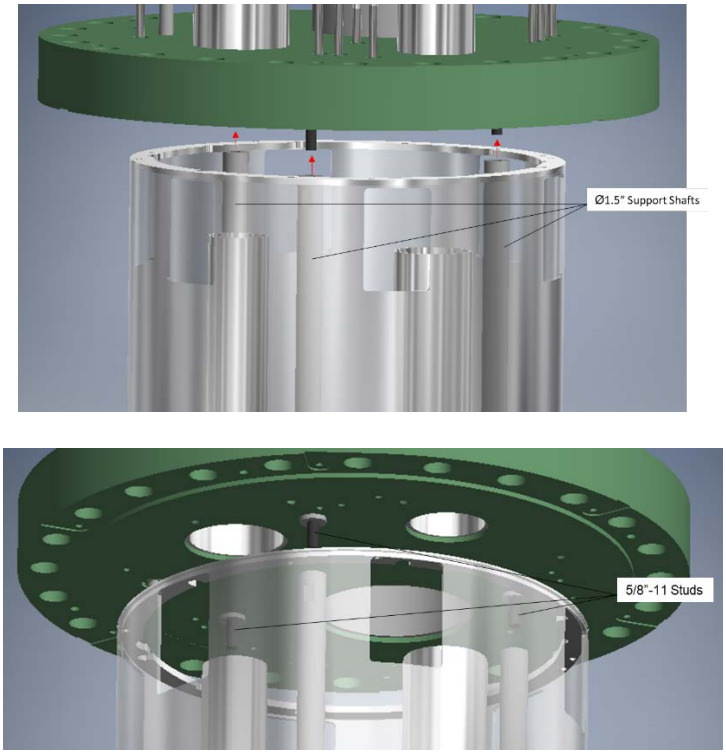

Figure 17: Drawing showing inner vessel offset from flange to illustrate support rod mounting location for inner vessel, top, mounting locations with studs installed in primary flange for support rods, bottom.

As can be seen in Figure 18, the primary flange was positioned on the CNC mill to drill and tap the 5/8-11” Helicoil threads for the support shafts. Figure 19 shows the inner vessel mounted to a CNC machine to drill the 3 mounting holes for the support shafts and to remove 1/16” of material off of the top ring of the inner vessel to elminiate contact between the inner vessel and the primary flange.

Figure 18: Primary flange positioned to bore 3X holes for 5/8" -11 STI tap for Nitronic-60 helicoil thread inserts to mount inner vessel support shafts

Figure 19: Inner vessel mounted to CNC machine for modifications

Figure 20 is a photo from inside the bottom of the inner vessel showing the three 1.5" diameter support shafts and Figure 21 is a photo of THETA dry assembly near completion.

Figure 20: Photo from inside the bottom of the inner vessel looking up towards the primary flange, the support shafts, intermediate heat exchanger shell and column pipe for the centrifugal pump are visible

Figure 21: Photo of THETA after dry assembly and prepared for water testing

3.2. Instrumentation

Table 3 summarizes THETA instrumentation which includes single and multi-point thermocouples, distributed optical fiber temperature sensors, and flowmeter voltage measurements. The port locations on the top flange have been labeled in Figure 22.

Table 3: THETA instrumentation and measurement. Port positions provided in Figure 22

Port #	Instrument	Measurement
1	Single TC	Heater inlet temperature
2	Single TC	Heater outlet temperature
3	Fiber	Hot and cold pool temperature
4	Rake TC	Hot and cold pool temperature
5	Rake TC	IHX outlet temperatures
6	Rake TC	Hot and cold pool temperature
7	Fiber	Hot and cold pool temperature
8	Rake TC	Outside inner vessel cold pool temperature
9	Rake TC	Hot and cold pool temperature
10	Fiber	Hot and cold pool temperature
11	MI Cable	Flowmeter voltage
12	Single TC	Flowmeter temperature
13	Fiber	Hot and cold pool temperature
14	Fiber	IHX temperature
15	Rake TC	IHX temperature
16-20	Single TCs	Heater temperatures, 3” above inlet

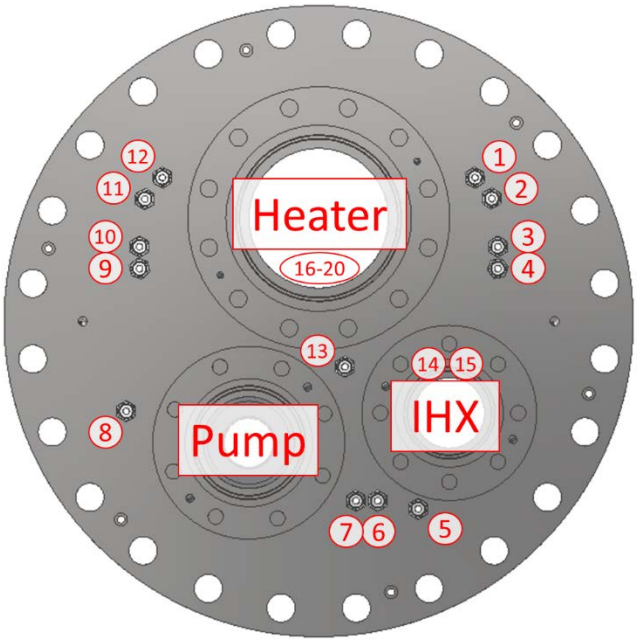

Figure 22: THETA instrumentation port locations

Port # 4, 6, and 9 possess 1/4" OD, 25-junction, k-type ungrounded thermocouple probes. The junctions possess a pitch of 2.375" and capture hot and cold pool axial temperatures with high fidelity, Figure 23.

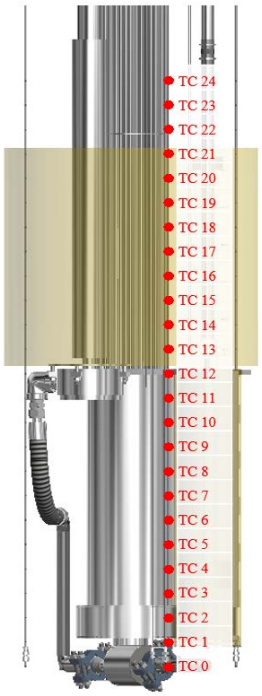

Figure 23: Multi-junction TC positions for ports 4, 6, and 9, hot pool sodium shown with translucent yellow for reference.

A photo of the multi-junction TC probes installed into ports 4 and 6 can be found in Figure 24. A photo of the three multi-junction TC probes in the cold pool region can be found in Figure 25.

Figure 24: Multi-junction TC probe installed in port #6, left. Multi-junction TC probe installed in port #4, right.

Figure 25: Dry fitting of THETA cold pool components in preparation for testing in deionized water. Multi-junction TC probes installed in ports # 4, 6, and 9 can be seen.

Optical fiber temperature sensors will be used to acquire distributed temperature data at spatial resolutions down to 0.65 mm and measurement rates of up to 250 Hz. These sensors are constructed from single mode silica fibers, Figure 26. An ODISI 6104 optical fiber interrogator system has been purchased and received from Luna Innovations, manufacturer specifications provided in Table 4.

.

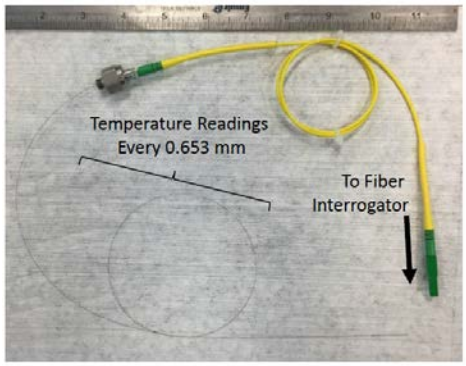

Figure 26: Photo showing 150 µm OD silica optical fiber

Table 4: ODISI 6104 spatial resolution and measurement rate

Spatial Resolution [mm]	Measurement Rate [Hz]
0.65	62.5
1.3	125
2.6	250

Optical fibers will be sheathed in a protective 1/16” OD 0.009” wall, 316 stainless steel capillary tube to protect them from sodium. Given there are no connection points for the 1/16” capillaries at the base of the 28” METL vessel, the optical fiber capillaries in ports 3, 7, and 10 will be mechanically attached to 1/4” multipoint thermocouple probes in ports 4, 6, and 9 to provide support, Figure 27 and Figure 28.

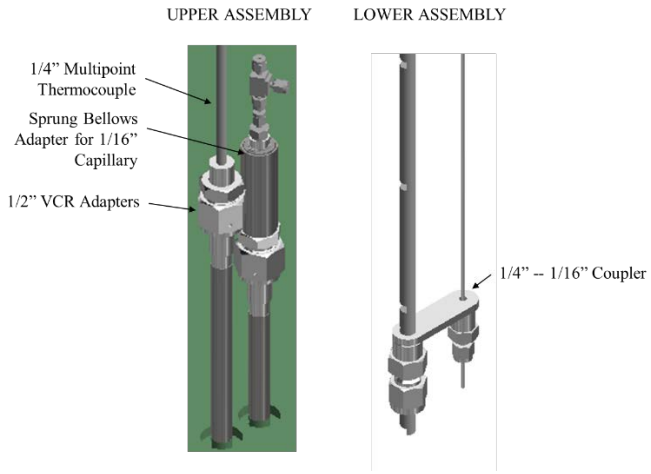

Figure 27: Optical fiber capillaries mechanically coupled to 1/4" multi-junction thermocouples

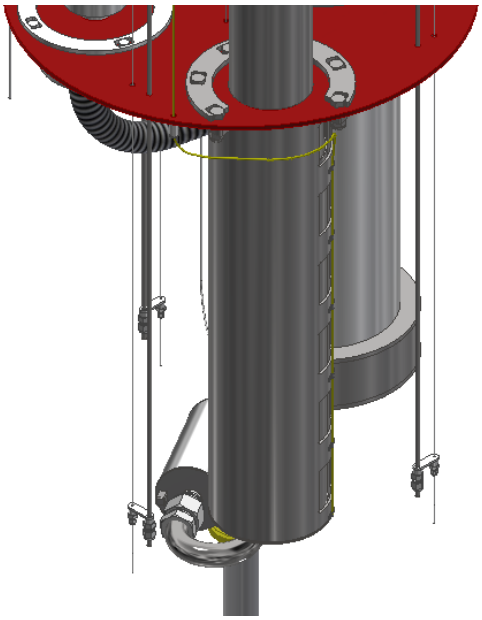

Figure 28: View of 3 optical fiber capillaries coupled to 1/4" multipoint thermocouple probes

A custom sprung bellows assembly has been designed to provide tension and to make up any thermal expansion differential between the 1/16" capillary tubes in ports 3, 7, 10, 13, and 14 and the rest of the primary vessel components, Figure 29. A complete description of the design can be found in [1]. A photo of the sprung bellows adapter installed in port #7 on the primary flange can be found in Figure 30.

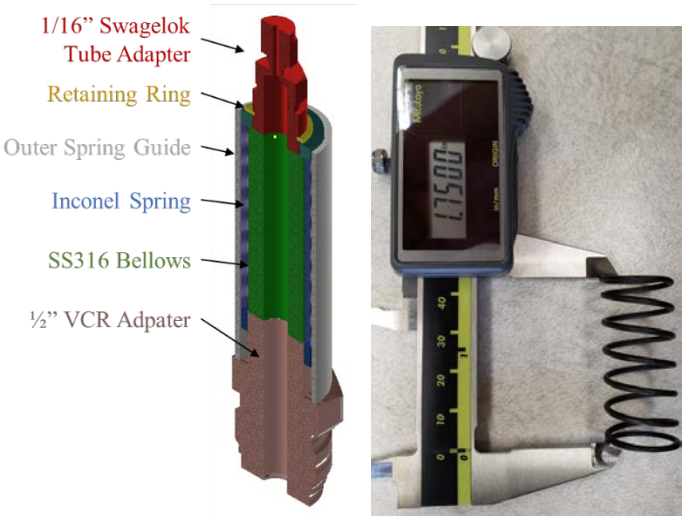

Figure 29: Sprung bellows to makeup thermal expansion differential of 1/16" capillaries, left. High temperature Inconel spring photo, right.

Figure 30: Sprung bellows adapter installed in port #7

3.3. Intermediate Heat Exchanger

An intermediate heat exchanger (IHX) has been designed to transfer heat from the THETA primary sodium to its secondary sodium system. As can be seen in Figure 31, the current design is a shell and tube type, with primary sodium on the shell side, and secondary sodium that flows through a tube bundle up-comer. Baffles with a ~1/2 shell window cross section are used to promote thermal mixing in the primary sodium. The down-comer sodium on the secondary side flows through a vacuum insulated tube. This is representative of typical SFR designs where the coldest sodium is delivered to the bottom of the intermediate heat exchanger to provide a counter-flow heat exchange. Two expansion bellows on the downcomer tube, one in the vacuum region and one above the vacuum region, accommodate thermal expansion differentials in the IHX. The design facilitates a 1/2" rod running concentric down the length of the shell to allow for adjustment of the IHX primary sodium outlet elevation into the cold pool, as will be discussed in a later section.

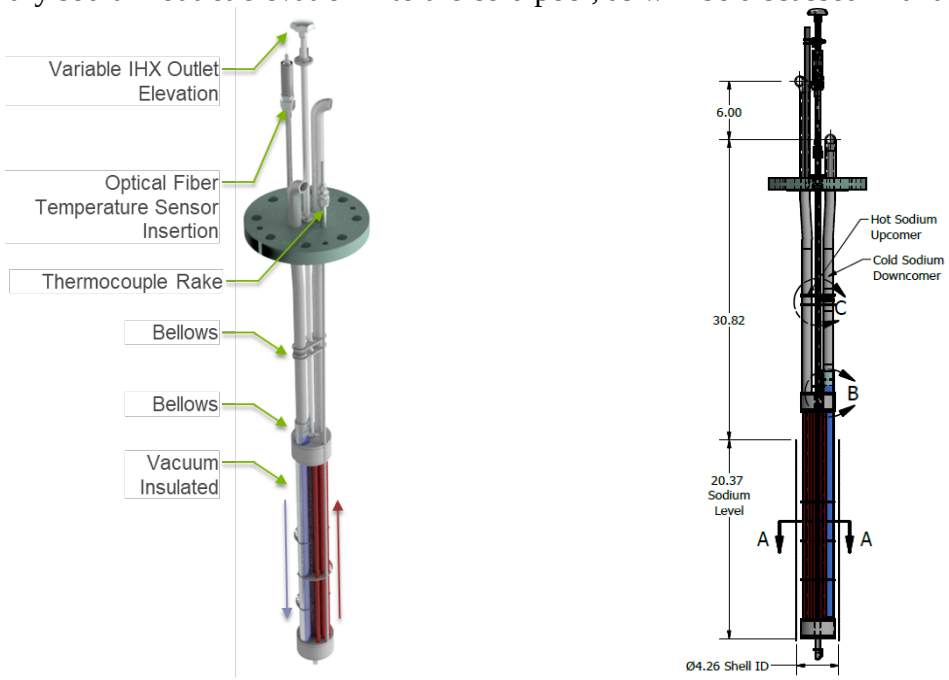

Figure 31: Shell and tube intermediate heat exchanger

Figure 32: Drawings showing IHX baffle plate and tube bundle upcomer

The heat exchanger was sized using the effectiveness-NTU method for one shell pass and a tube bundle pass. This method identifies the maximum possible heat transfer rate and uses a calculated effectiveness to determine the actual heat transfer rate, Eq. 1.

$$\dot{q} = \varepsilon \dot{q}_{max} \tag{1}$$

The effectiveness for a heat exchanger of this type as a function of transfer units and capacity ratio can be found in Eq. 2.

$$\varepsilon = \begin{cases} \dfrac{1 - \exp\left[-NTU\,(1 - C_R)\right]}{1 - C_R \exp\left[-NTU\,(1 - C_R)\right]} & \text{for } C_R < 1 \\ \dfrac{NTU}{1 + NTU} & \text{for } C_R = 1 \end{cases} \tag{2}$$

Where C_R is a dimensionless number referred to as the capacity ratio, comparing the capacitance rates of the tube and the shell side fluids, Eq. 3, and NTU is the number of transfer units, calculated using Eq. 4.

$$C_R = \frac{\dot{C}_{min}}{\dot{C}_{max}} \tag{3}$$

Where $\dot{C}_{min}$ and $\dot{C}_{max}$ are the minimum and maximum of the capacitance rates of fluid on either side of the heat exchanger.

$$NTU = \frac{UA}{\dot{C}_{min}} \tag{4}$$

The conductance of the heat exchanger, UA, is a function of both geometry and heat transfer in the heat exchanger. The conductance may be found by taking the inverse of the total thermal resistance, Eq. 5.

$$UA = \frac{1}{R_{tot}} = \frac{1}{R_{h,tube} + R_k + R_{h,shell} + R_f} \tag{5}$$

Where $R_{h,tube}$ is the convection resistance from the tube fluid to the tube inner wall, R_k is the resistance to conduction in the tube wall, $R_{h,shell}$ is the convection resistance from the shell fluid to the tube outer wall, and R_f is the resistance due to fouling. According to literature the fouling resistance in alkali metal heat exchangers is negligible if oxide level is kept below a few wppm [5]. The convection resistance may be determined with the use of the Nusselt number. On the tube side, the Nusselt number was found using a correlation for NaK flowing through a tube [6], Eq. 6.

$$Nu = 4.82 + 0.0185 \cdot Pe^{0.827} \tag{6}$$

On the shell side, the Nusselt number was found using a correlation for in-line flow through un-baffled rod bundles in wide spaced arrays (tube pitch / tube diameter = P/D > 1.35) [7], Eq. 7. Note that P/D for the above THETA IHX is 1.73.

$$Nu = 6.66 + 3.126\frac{P}{D} + 1.84\left(\frac{P}{D}\right)^2 + 0.0155(\bar{\varphi}Pe)^{0.86} \quad (7)$$

Where $\bar{\varphi}$, the ratio between eddy diffusivities of heat and momentum, is generally assumed equal to one [8].

Using the thermal hydraulic parameters given in Table 5, the performance of the THETA IHX may be predicted. As can be seen, the secondary sodium system flowrate was set to 5 GPM, the primary sodium inlet temperature was set to 550 °C, the secondary sodium inlet temperature was set to 450 and 500 °C. The shell side temperature differential and thermal power dissipation as a function of shell side flow rate can be found plotted in Figure 33.

Table 5: Intermediate heat exchanger sizing parameters

Parameter	Value	Unit
$Q_{sodium,secondary}$	5	GPM
$T_{sodium,primary,in}$	550	°C
$T_{sodium,secondary,in}$	450, 500	°C

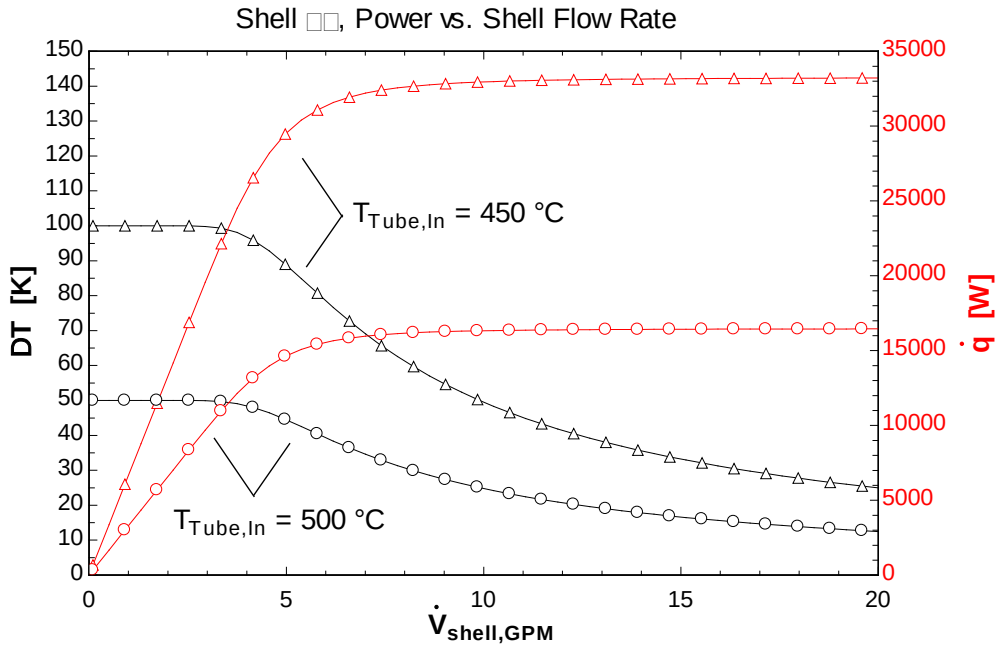

Figure 33: IHX predicted shell side temperature differential and thermal power dissipation as a function of shell side flow rate

The IHX possesses a variable height outlet mechanism allowing for exiting of cold sodium at various elevations in the cold pool to study the transient and steady state temperature profile which develop throughout an SFR as a result of changing this variable, Figure 34. Depositing cold sodium

at a lower elevation in the cold pool is predicted to result in more stratification and ultimately result in a more thermally stratified hot pool. This will be an important variable to study for the development of reactor codes. Figure 35 shows drawings of the inner and outer barrel. As can be seen there are qty. (6) 2.75” square windows at elevations spaced 4.5” apart from center to center. The inner barrel rests on a stainless steel cone on the bottom of the outer barrel in a Hastelloy C-276 seat, reducing the likelihood of galling. A photo showing the finished IHX outlet inner and outer barrel can be seen in Figure 36. The IHX outlet can be seen installed onto THETA in Figure 21.

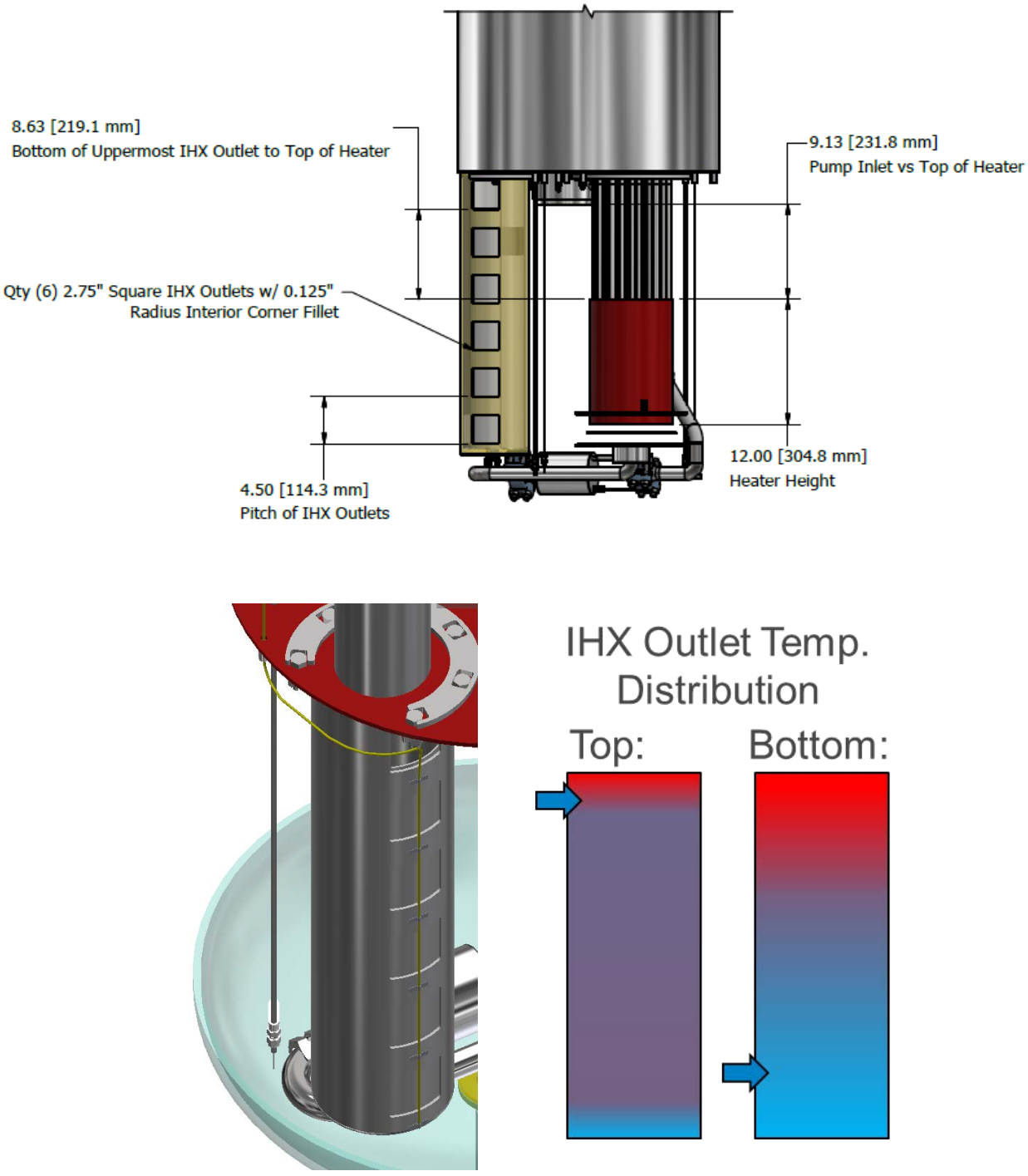

Figure 34: IHX Outlet dimension, top. Isometric model of variable elevation IHX outlet, bottom left. Drawing showing predicted cold pool temperature distribution as a function of IHX outlet window elevation, (red = hot, purple = warm, blue = cold), bottom right.

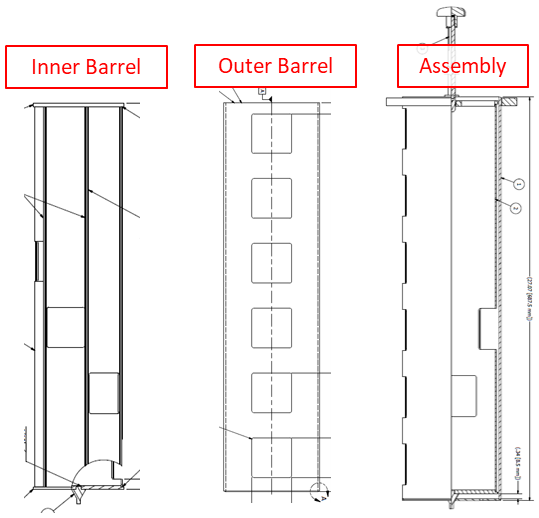

Figure 35: Variable elevation IHX outlet. Drawings showing the inner barrel, left, outer barrel, middle, and the assembly of inner/outer barrel and actuator stem, right.

Figure 36: Photo showing the IHX outlet inner barrel, left, and the outer barrel, right

3.4. Submersible Flowmeter

A submersible permanent magnet flowmeter has been designed to acquire primary sodium flowrate, Figure 37. The flowmeter uses a magnetic field generated by high temperature Samarium-Cobalt (SmCo) magnets, oriented perpendicular to sodium flow, to generate a Lorentz current that is linearly proportional to flow. A complete description of the design and construction of the flowmeter can be found in [1]. A photograph of the completed flowmeter can be found in Figure 38. Flowmeter calibration in a sodium loop is planned to verify theoretical voltage vs flowrate curve predicted by theory, Figure 39.

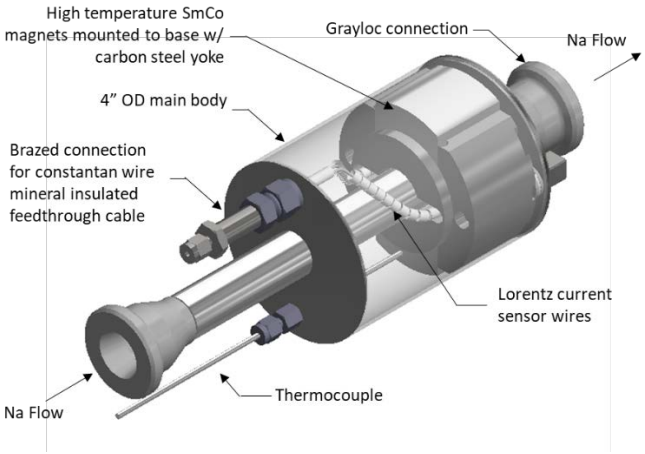

Figure 37: Submersible permanent magnet flowmeter

Figure 38: Photo of the THETA submersible permanent magnet flowmeter

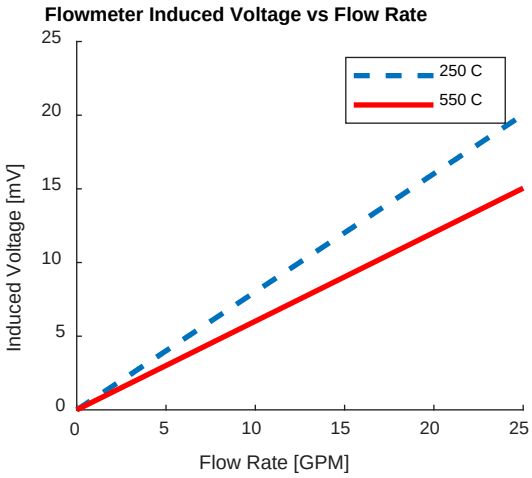

Figure 39: Flowmeter induced voltage vs flow rate for THETA submersible electromagnetic flowmeter, [1]

3.5.**Pump**

The primary sodium centrifugal pump has been received from Wenesco Inc., Figure 40. The flow curve for the pump using deionized water can be found in Figure 41 [1].

Figure 40: Pump as delivered, left, 4.5" OD impeller, right.

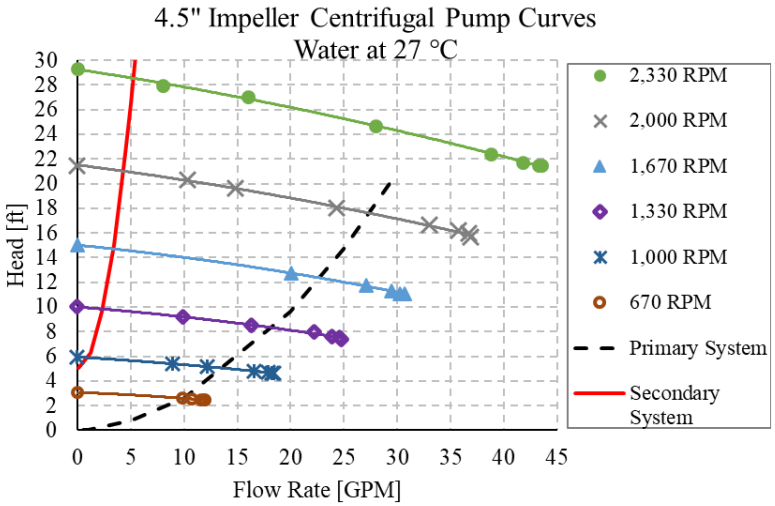

Figure 41: Pump curves made using water at 27 °C as surrogate fluid. System curves shown for primary and secondary sodium.

A photo of the air-to-sodium seal for the centrifugal pump shaft can be found in Figure 42. As can be seen it consists of a packing block that houses three layers of 1/2" square high speed packing cord made with expanded-graphite yarn with carbon yard corners. After installing the first layer of packing a lantern ring is installed that acts to trap a layer of pressurized inert gas between the first layer and the second and third layers of packing, Figure 43 and Figure 44. This ensures a hermetic seal for the cover gas in the sodium as the inert gas void space provided by the lantern ring can be regulated at a slightly higher pressure than the sodium cover gas, limiting cover gas egress or air ingress into the system.

Figure 42: Photo showing the air-to-sodium seal for the THETA centrifugal pump. Shown from left to right: packing block, lantern ring, follower.

Figure 43: Photo showing the 5” 300# ANSI flange with graphite gasket in place in preparation for installation of packing block. Nitronic-60 helicoil thread adapters are installed in all threads to reduce likelihood of galling.

Figure 44: Photo showing the packing block cavity. On the right can be seen a single layer of graphite packing. Two holes are bored radially into the cavity, the lower one shown is for inert gas pressurization of the lantern ring void, the upper bore is for an 1/8” thermocouple to monitor packing temperatures during operation.

A debris 'thrower' is mounted below the pump flange on the shaft, Figure 45. This thrower catches any graphite debris that may be shed from the seal above. As the shaft spins, the debris is deposited into a debris well below, Figure 46, Figure 47.

Figure 45: Photo showing the wetted face of the pump flange along with the thrower that acts to centrifugally deposit debris falling from the packing block into the debris well. Also notice the ethanol, this is sprayed onto lint-free lab wipes and used to ensure cleanliness of all components before testing.

Figure 46: Photo showing the 5" 300# mounting flange on the THETA primary flange. The energized spring seal groove can be seen on the raised face. A debris well can be seen which acts to catch any dust or large particles that may fall from the graphite packing seal.

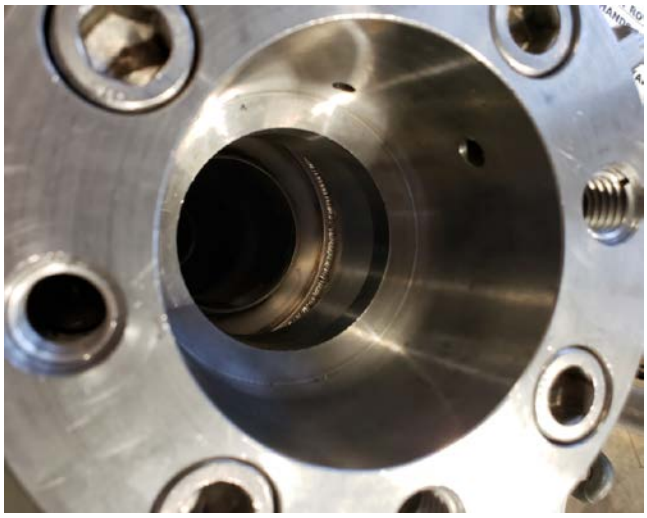

Figure 47: Photo showing the packing block installed with the debris well below.

A labyrinth seal consisting of a bottom plate that is sandwiched between the case and the inner vessel and a shaft adapter was added to reduce flow from out of the top of the pump case, Figure 48 and Figure 49. The pump shaft does not possess a lower bearing; thus a contact free seal is required to reduce unwanted sodium egress out of the top of the case, into the hot pool. The labyrinth seal works by introducing a serpentine path which increases the pressure differential, thus reducing flow.

Figure 48: Photo showing the centrifugal pump case with labyrinth seal lower plate and shaft adapter.

Figure 49: Photo showing the labyrinth seal shaft adapter

The assembled pump was installed on to the primary vessel, Figure 50, and labyrinth seal and impeller installed onto the bottom of the shaft afterwards, Figure 51. Figure 52 shows the completed lower pump assembly with case and piping installed.

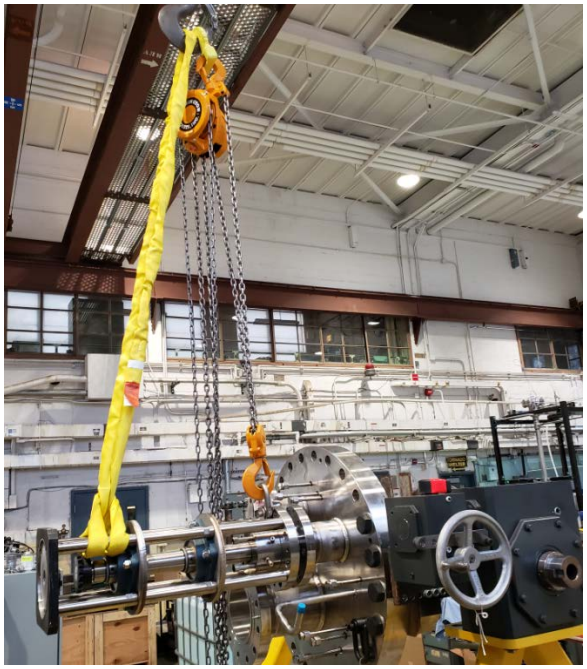

Figure 50: Photo showing the installation of the centrifugal pump shaft and upper bearing assembly into THETA.

Figure 51: Photo showing the bottom side of the inner vessel, pump case is not installed so the labyrinth plate and pump impeller are visible

Figure 52: Photo showing the underside of the inner vessel with pump case and piping installed

Colleagues at Oak Ridge National Laboratory have 3D printed a 316L pump impeller that will be tested in the future on THETA to assess the long term reliability of this technology in a critical sodium component, Figure 53 [9].

Figure 53: 4.5" Diameter 316SS 3D printed impeller by Oak Ridge National Laboratory, [9]

3.6. Immersion Heater

The immersion heater and associated electrical enclosure have been received from Chromalox, Figure 54. Heater elements were tested with a multimeter to ensure proper rated resistance of ~35 ohms, indicating no significant damage occurred during shipment. The immersion heater is currently installed on the THETA primary flange, Figure 55. A photo showing one of four over temperature thermocouples welded to the Incoloy sheath. A process control thermocouple, not shown, is located at the center of the bundle. A photo showing the immersion heater shroud, which surround the heater to form the core, can be found in Figure 57.

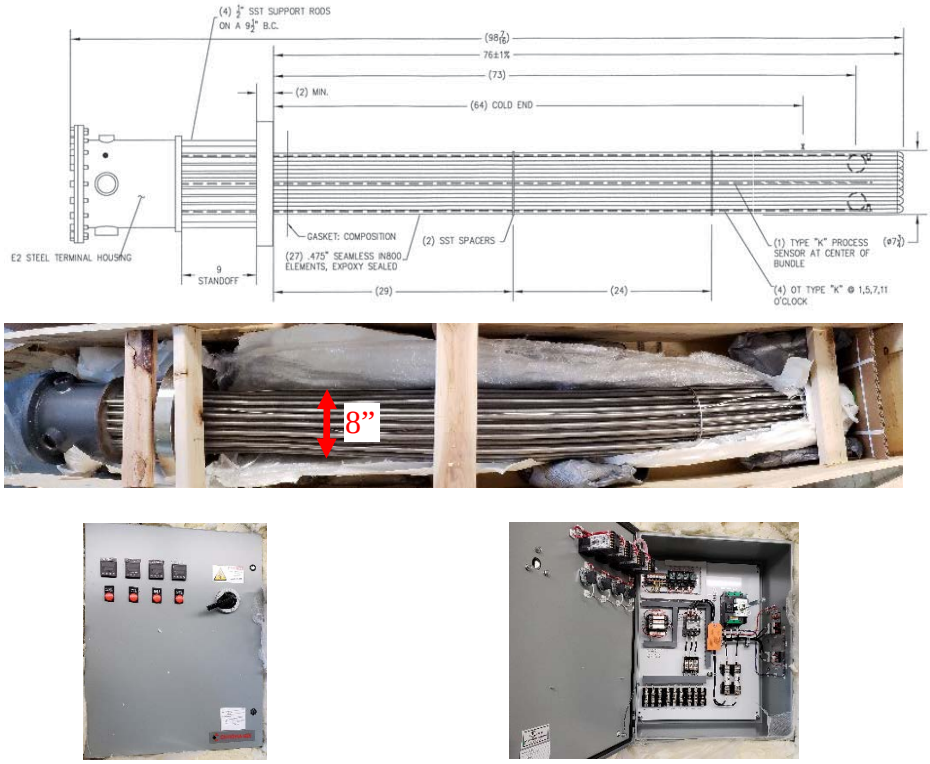

Figure 54: Chromalox 38 kW Immersion Heater (top). Heater control system electrical enclosure (bottom).

Figure 55: Photo showing the installation of the THETA immersion heater.

Figure 56: Photo showing two of the four thermocouples welded to the hairpin heaters at the bottom of the immersion heater

Figure 57: Photo showing the shroud that surrounds the immersion heater in the cold pool to form the core flow path

4. Secondary Sodium Component Summary

This section provides an update for the THETA secondary sodium components and piping. A 3D isometric drawing of the current secondary system design can be found in Figure 58. As can be seen an AC Conduction based electromagnetic pump pushes sodium through an air-to-sodium heat exchanger, a permanent magnet flowmeter, and an intermediate heat exchanger.

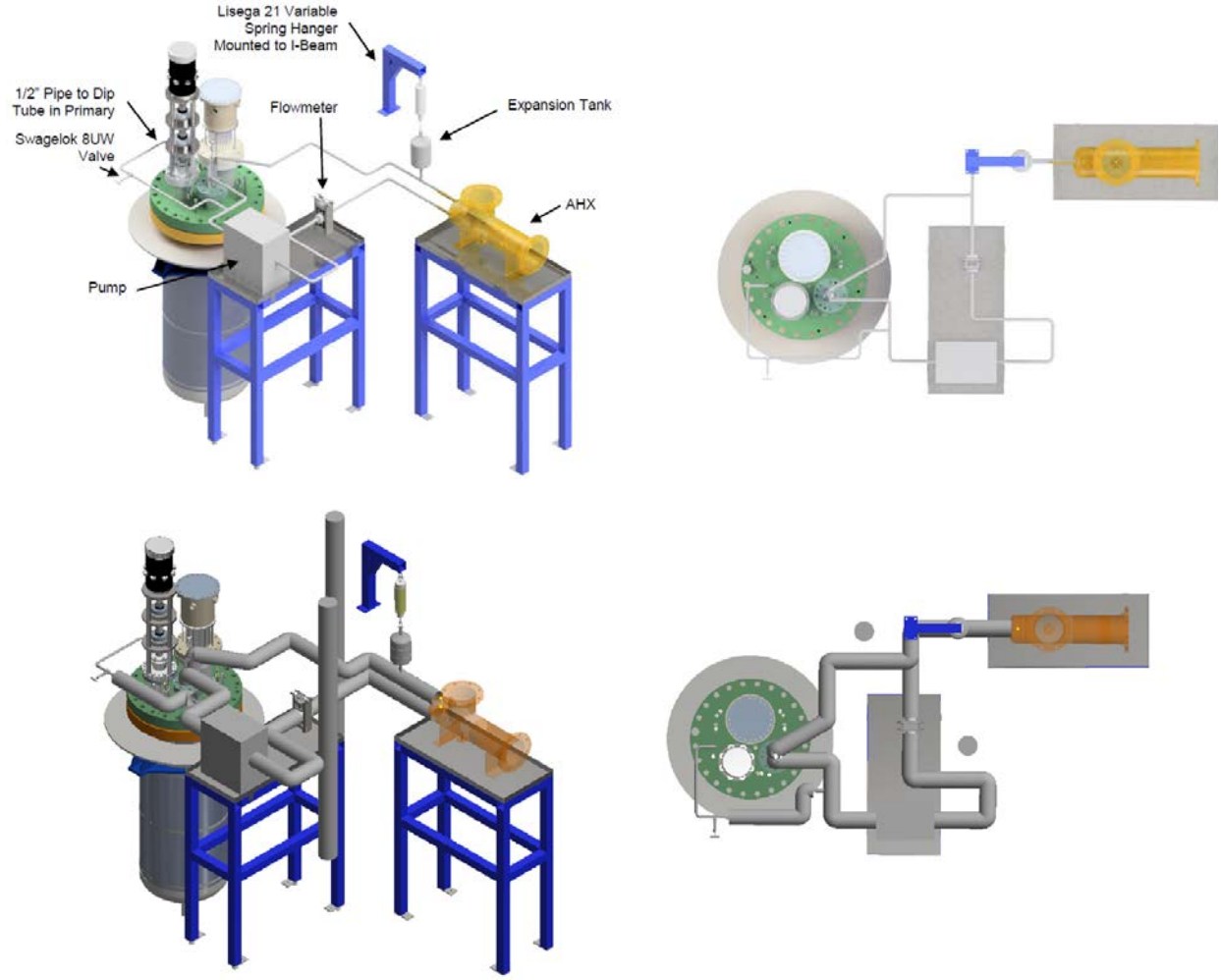

Figure 58: Isometric 3D drawing showing THETA secondary system without (top) and with (bottom) 2" of insulation

4.1. Sodium-to-Air Heat Exchanger

A custom, U-stamped (ASME BPVC Sec. VIII Div. 2) air to sodium heat exchanger was constructed at Enerquip LLC in Medford, Wisconsin. The heat exchanger is a tube and shell design, with sodium flowing through qty. (24), 0.75" OD x 0.049" wall, 24" long single pass seamless 316/316L SS U-tubes. The heat exchanger bonnet, tube sheet, tubes, and shell were fully welded with RT1 radiography, hydrostatic pressure test, and helium leak check to ensure no egress of sodium during operation. The heat exchanger is rated for a maximum sodium temperature of 538 °C (1000 °F) at 100 PSIG with a maximum heat dissipation of 39 kW (133.8 kBtu/hr).

A photo of the sodium-to-air heat exchanger can be found in Figure 59. A summary of the heat exchanger sizing analysis from the manufacturer has been provided in Table 6.

Figure 59: Photo of the sodium-to-air heat exchanger as received from the manufacturer

Table 6: Sodium-to-Air heat exchanger specification sheet

HEAT EXCHANGER SPECIFICATION SHEET — Page 1 — **US Units**

							Job No.				
Customer	Argonne National Laboratory						Reference No.	Matt Weathered			
Address							Proposal No.	51156R2			
Plant Location	Argonne, IL 60439						Date	5/31/19		Rev	
Service of Unit	Cooler						Item No.				
Size	8.329 x 24	inch	Type	BEU	Vertical		Connected In	1	Parallel	1	Series
Surf/Unit (Gross/Eff)	19.218 / 18.678	ft2	Shell/Unit	1			Surf/Shell (Gross/Eff)	19.218 / 18.678	ft2		

PERFORMANCE OF ONE UNIT

Fluid Allocation		Shell Side		Tube Side	
Fluid Name		1200 SCFM Air		5 gpm Liquid Sodium	
Fluid Quantity, Total	lb/hr	5400.0		2102.0	
Vapor (In/Out)		5400.0	5400.0		
Liquid				2102.0	2102.0
Steam					
Water					
Noncondensables					
Temperature (In/Out)	F	77.00	180.12	1000.0	790.00
Specific Gravity				0.8262	0.8533
Viscosity	cP	0.0186	0.0212	0.2240	0.2670
Molecular Weight, Vapor					
Molecular Weight, Noncondensables					
Specific Heat	Btu/lb-F	0.2390	0.2416	0.3009	0.3055
Thermal Conductivity	Btu/hr-ft-F	0.0151	0.0176	36.044	39.482
Latent Heat	Btu/lb				
Inlet Pressure	psia	16.496		24.696	
Velocity	ft/sec	84.12		0.22	
Pressure Drop, Allow/Calc	psi	10.000	0.782	10.000	0.036
Fouling Resistance (min)	ft2-hr-F/Btu	0.00050		0.00200	

Heat Exchanged	133830	Btu/hr		MTD (Corrected)	760.1	F
Transfer Rate, Service	9.43	Btu/ft2-hr-F	Clean 20.50	Btu/ft2-hr-F	Actual 19.39	Btu/ft2-hr-F

CONSTRUCTION OF ONE SHELL

Sketch (Bundle/Nozzle Orientation)

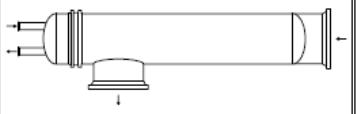

			Shell Side	Tube Side
Design/Test Pressure		psig	50.000 /	50.000 /
Design Temperature		F	250.00	1000.0
No Passes per Shell			1	2
Corrosion Allowance		inch	0.0000	0.0000
Connections	In	inch	1 @ 8.0000	1 @ 1.0000
Size &	Out	inch	1 @ 8.0000	1 @ 1.0000
Rating	Intermediate		@	@

Tube No.	22U	OD	0.7500	inch	Thk(Avg)	0.0490	inch	Length	2.000	ft
Pitch	0.9375	inch								
Tube Type	Plain				Material	SA-213 TP304L Tube (S) S30403				
Tube pattern	60									
Shell	SA-312 TP304L Pipe (W) S30403	ID	8.3290	OD	8.6250	inch	Shell Cover			(Integ.)
Channel or Bonnet	SA-240 304L Pl. S30403						Channel Cover			
Tubesheet-Stationary	SA-240 304L Pl. S30403						Tubesheet-Floating			
Floating Head Cover							Impingement Plate	None		
Baffles-Cross		Type	None		%Cut (Diam)		Spacing(c/c)	25.944	Inlet	inch
Baffles-Long					Seal Type	None				
Supports-Tube					U-Bend				Type	None
Bypass Seal Arrangement	0	pairs seal strips			Tube-Tubesheet Joint	Expanded and seal welded (2 grooves)				
Expansion Joint					Type					
Rho-V2-Inlet Nozzle	222.48	lb/ft-sec2			Bundle Entrance	0.00	Bundle Exit	0.00	lb/ft-sec2	
Gaskets-Shell Side					Tube Side					
- Floating Head										
Code Requirements	ASME						TEMA Class	C		
Weight/Shell	239.92	lb	Filled with Water	337.60	lb		Bundle	67.49	lb	

Remarks (cont.) — Page 2
316/316L SA-213 seamless tubes. All 304/304L for remaining Tube Side Components
All 304/304L Shell Side Components
Industrial Finish: All surfaces are as machined or mill finish with welds cleaned to remove discoloration where accessible.
All Welded tubesheet and bonnet. Non removable.
NPS 300# ANSI Flange Tube Side Connections
NPS 150# ANSI Flange Shell Inlet
NPS 150# ANSI Flange Shell Outlet
NPT 3000# Coupling Shell Vent
U-Stamped
No China or India materials preferred. Acceptable from Japan, Europe, Canada, Domestic.
Passivation included
3.164 gallons for tubeside holdup

4.2. Secondary Sodium Piping

A thermal stress analysis was performed with CAESAR II computer software to ensure safe operation during all potential operating conditions. The piping analysis demonstrated passing of ASME B31.3 pipe code under all extreme and nominal operating conditions.

The secondary piping system is seamless 3/4" SCH 40 piping made with 316H stainless steel (ASTM 376 type 316H) given its superior strength at high temperature as compared to other grades of 300 series stainless. All of the fittings are 3/4" SCH 40 316/316L seamless tubes. Originally the fittings were specified as 316H, however during procurement it was found that these were not readily available from a domestic or DFARS (Defense Federal Acquisition Regulation Supplement) compliant supplier. 316/316L (ASTM A182 Type F316 or ASTM A403 Type WP316) possesses the same strength rating as 316H up to and including 1000 °F and is more readily available, therefore the fittings were specified using this grade of stainless.

The maximum temperature limit of the system is 538 °C (1000 °F) and the system has a design pressure of 50 PSIG. A total of six scenarios were identified for analysis to bound all possible operating conditions:

1. Filling system at 200 °C (392 °F)
2. System at maximum temperature, all piping and vessel at 538 °C (1000 °F)
3. IHX and AHX on, cold leg pump direction, 421 °C (790 °F) to 538 °C (1000 °F) ΔT
4. IHX and AHX on, hot leg pump direction, 421 °C (790 °F) to 538 °C (1000 °F) ΔT
5. Cold condition, system at 32 °C (0 °F)
6. Scenario #2 with seismic analysis

A screenshot of the CAESAR-II software setup to test Scenarios 1-6 can be found in Figure 60.

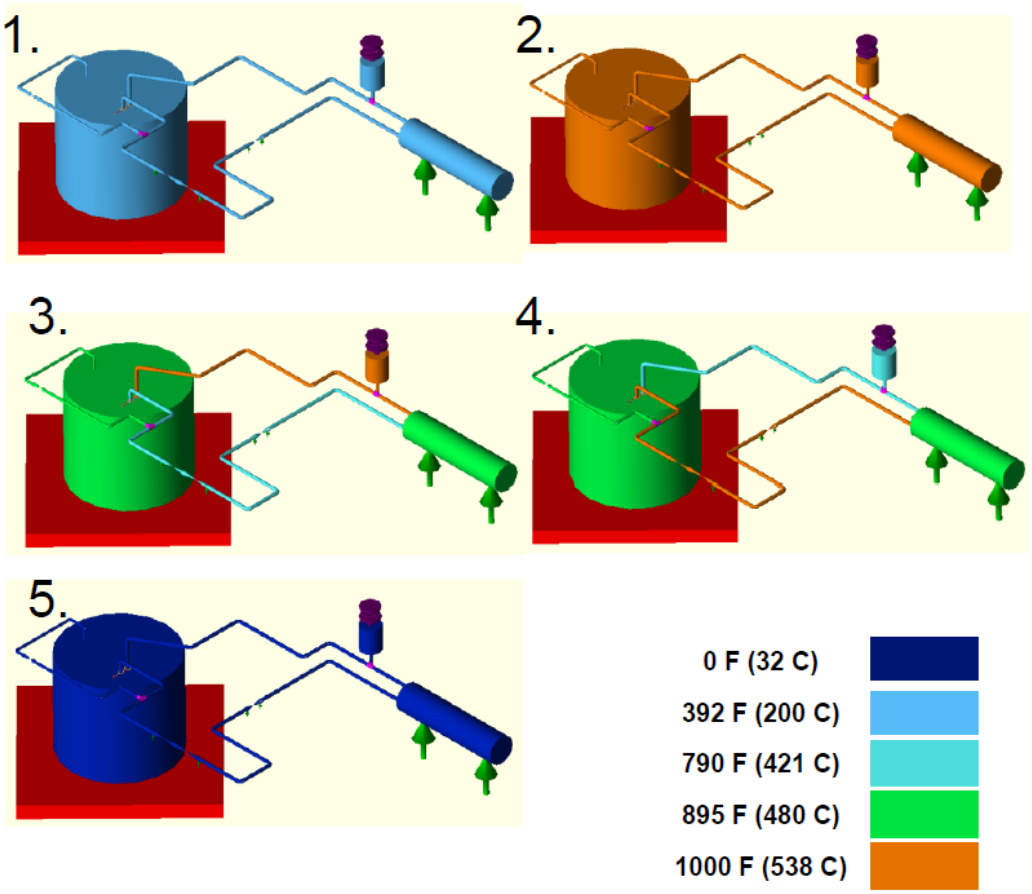

Figure 60: CAESAR operating scenarios showing vessel, AHX, expansion tank, piping temperatures

5. WATER TESTING

Water has been shown to be a good surrogate for sodium when performing thermal hydraulic experiments, possessing very similar density and viscosity to within an order of magnitude. In fact, water possesses some favorable characteristics over sodium when simulating certain thermal hydraulic phenomena with a small scale experiment; water has a reduced thermal conductivity resulting in a larger Pe number for a small scale experiment, allowing for more representative temperature gradients when simulating thermal stratification in a pool type SFR [3]. All of the THETA components will function in water except for the electromagnetic flowmeter. Therefore, the flowmeter described in Section 3.4 has been replaced with a Blancett B110-875, 3-30 GPM turbine mechanical flowmeter.

A 36” diameter, 60” tall, 260 gallon polypropylene vessel (PN: Chem-Tainer TC6330AB) was acquired for water testing of THETA, Figure 61. The vessel has a maximum temperature limit of 100 °C. A dip tube constructed with PVC supplies water and will drain water from the vessel with a self-priming pump assembly, Figure 61. The self-priming pump is a 1/3-HP centrifugal pump

with 41 ft max head (PN: Dayton 5GUP0). All wetted materials in the pump are compatible with deionized water (stainless steel, viton, carbon, ceramic). A 275 gallon intermediate bulk container is used to store the deionized water, Figure 62. The valve manifold shown in Figure 63 makes the water transfer a closed system, allowing the user to select water flow to or from the test vessel, thus conserving the deionized water between tests if the experiment must be drained, and reduces the chance of a gross leak of water.

Figure 61: 260 gallon polypropylene vessel for THETA water testing, left. Dip tube for transferring DI water between the intermediate bulk container and the polypropylene vessel, right.

Figure 62: 275 gallon intermediate bulk container of deionized water, left. Self-priming pump and valve manifold for transferring water between the intermediate bulk container and the test vessel.

In order to reduce biological (algae) growth in the deionized water, a UV filtration system was built. The manifold shown in Figure 63 attaches to the line from the intermediate bulk container and allows the user to throttle the water flow down to 6 GPM to expose the DI water to the UV lamp for sanitization.

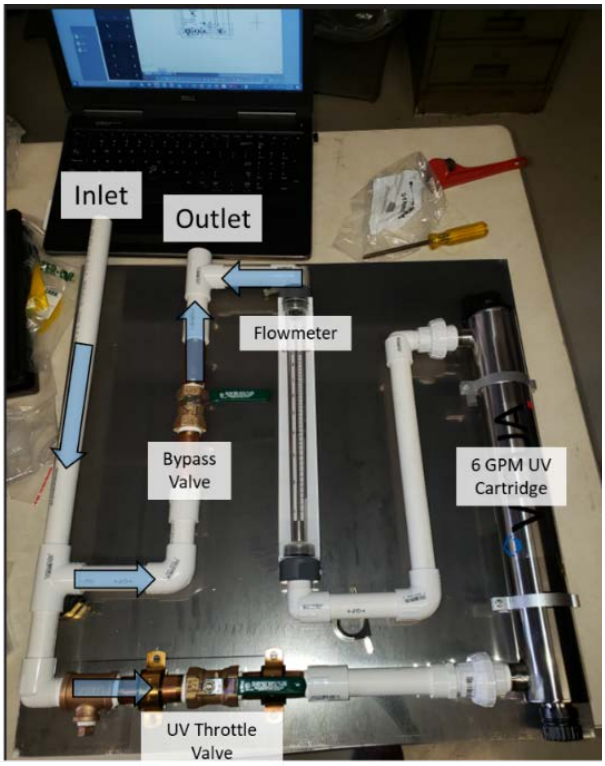

Figure 63: Manifold for ultraviolet sanitization of DI water to eliminate biological contamination. Water may be directed and through the UV cartridge with the UV Throttle Valve. The valve may be throttled to <=6GPM to ensure sufficient residency time of the flowing water to eliminate contaminates. A 0-10 GPM flowmeter is positioned in line with the UV cartridge circuit.

A Blancett B110-875, 3-30 GPM turbine mechanical flowmeter was installed in the system to acquire water flowrate, Figure 64. Photographs in Figure 65 show THETA installed on the yellow A-frame 'flipper' and surrounded by polypropylene vessel with multi-junction thermocouple probes plugged into gray umbilical boxes that feed data back to the data acquisition system. Also found in Figure 65 is a photo of the completed UV water sanitization system.

A pump shakedown has been performed of the assembled THETA, a plot showing flowrate as a function of pump speed can be found in Figure 66. The pump speed has been brought to a maximum speed of 1,771 RPM without any noticeable shaft runout that would cause vibration.

The pump was previously tested up to 2,330 RPM thus there is more performance attainable with this pump that will be explored with further shakedown testing.

The multi-junction thermocouple probes that acquire distributed temperature profiles in the hot and cold pool have all be connected to the data acquisition system and are ready to collect water testing data once the immersion heater has been put online. The immersion heater control box was mounted and accommodations have been made to provide power for the heater, final wiring of the immersion heater to the control box is required.

Figure 64: Photo of THETA bottom assembly ready for water testing, a Blancett PN B110-875 turbine mechanical flowmeter will be used for water testing, shown installed at the bottom with yellow colored waterproof data cable connected.

Figure 65: THETA installed in polypropylene vessel with all thermocouple instrumentation attached, left. Completed water UV purification system and 275-gallon intermediate bulk container, right.

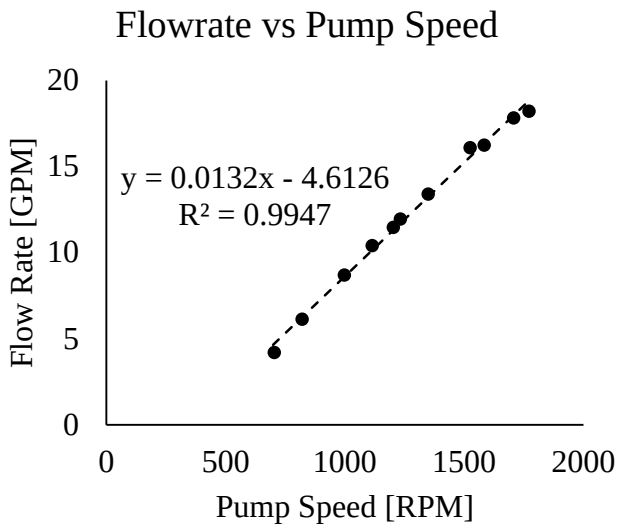

Figure 66: THETA pump shakedown preliminary results for flow rate as a function of pump speed. Water at room temperature (no immersion heater). Note that this data was taken without the shaft portion of the labyrinth seal installed, only the case lower plate portion, Figure 48.

6. THETA Model Development

Modeling of the Thermal Hydraulic Experimental Test Article (THETA) experiment has been performed using the SAS4A/SASSYS-1 fast reactor safety analysis code. A THETA model has been developed to represent the THETA experiment design developed at Argonne to demonstrate the importance of key elevations on natural circulation flow rates. The model currently includes the core channel and the primary heat transport system of the THETA experimental facility. A summary of this work can be found in [1].

7. Conclusions and Path Forward

All major components for the primary system have been acquired and dry assembled. The recent laboratory shut down due to COVID-19 has delayed water testing of THETA components but work is now proceeding and preliminary shakedown testing of the pump as installed in THETA is underway as of the publication of this report. Design work on the secondary system is nearing completion, the air-to-sodium heat exchanger is on site and ready for installation, this represents the longest lead time component so this will prevent delay when beginning secondary loop construction. Given the rigor of design work and safety analysis on the facility and the collaboration of designers with systems code developers, THETA will be an important asset for the METL facility and for sodium cooled reactor component and code development.

8. Acknowledgements

The authors would like to acknowledge the rest of the Mechanisms Engineering Test Loop (METL) team, Anthony Reavis and Daniel Andujar, for all of their hard work and dedication to constructing, maintaining and operating the facility. The authors would also like to acknowledge Dzmitry Harbaruk and Henry Belch for their assistance in monitoring METL systems during 24-hour operations. This work is funded by the U.S. Department of Energy Office of Nuclear Energy's Advanced Reactor Technologies program. A special acknowledgement goes to Mr. Brian Robinson, Fast Reactor Program Manager for the DOE-NE ART program and to Dr. Robert Hill, the National Technical Director for Fast Reactors for the DOE-NE ART program for their consistent support of the Mechanisms Engineering Test Facility and its associated experiments, including the Thermal Hydraulic Experimental Test Article (THETA). Prior years' support has also been provided by Mr. Thomas O'Connor, Ms. Alice Caponiti, and Mr. Thomas Sowinski of U.S. DOE's Office of Nuclear Energy.

9. References

[1] M. Weathered *et al.*, "Thermal Hydraulic Experimental Test Article – Status Report for FY2019 Rev. 1," Lemont, 2019.

[2] T. Sumner and A. Moisseytsev, "Simulations of the EBR-II Tests SHRT-17 and SHRT-45R," in *16th International Topical Meeting on Nuclear Reactor Thermal Hydraulics (NURETH-16)*, 2015.

[3] N. Tanaka, S. Moriya, S. Ushijima, and T. Koga, "Prediction method for thermal stratification in a reactor vessel," *Nucl. Eng. Des.*, vol. 120, pp. 395–402, 1990.

[4] M. T. Weathered, "Characterization of Sodium Thermal Hydraulics with Optical Fiber Temperature Sensors," 2017.

[5] W. Logie, C. Asselineau, J. Pye, and J. Coventry, "Temperature and Heat Flux Distributions in Sodium Receiver Tubes," no. December, 2015.

[6] E. Skupinski, J. Tortel, and L. Vautrey, "Determination des coefficients de convection d'un alliage sodium-potassium dans un tube circulaire," *Int. J. Heat Mass Transf.*, vol. 8, no. 6, pp. 937–951, 1965.

[7] Maresca and Dwyer, "Heat Transfer to Mercury Flowing In-Line Through a Bundle of Circular Rods," *Trans. ASME*, 1964.

[8] Foust, *Sodium-NaK Engineering Handbook Vol II*. 1979.

[9] K. Terrani, R. Dehoff, R. Duncan, and F. List, "Email Correspondence on 3D Printed Impeller with ORNL." 2020.

Nuclear Science and Engineering
Argonne National Laboratory
9700 South Cass Avenue, Bldg. 208
Argonne, IL 60439

www.anl.gov

Argonne National Laboratory is a U.S. Department of Energy laboratory managed by UChicago Argonne, LLC